Geomechanics and Engineering, *Vol. 30, No. 1 (2022) 67-73*
https://doi.org/10.12989/gae.2022.30.1.067

Fiber orientation distribution of reinforced cemented Toyoura sand

Muhammad Safdar*[1], Tim Newson[2a] and Muhammad Waseem[3]

[1]*Earthquake Engineering Center, Department of Civil Engineering, University of Engineering and Technology Peshawar, Pakistan*
[2]*Department of Civil and Environmental Engineering, Western University, London, Ontario, Canada*
[3]*Department of Civil Engineering, University of Engineering and Technology Peshawar, Pakistan*

(Received November 25, 2020, Revised May 23, 2022, Accepted June 7, 2022)

Abstract. In this study, the fiber orientation distribution (FOD) is investigated using both micro-CT (computerized tomography) and image analysis of physically cut specimens prepared from Polyvinyl Alcohol (PVA) fiber reinforced cemented Toyoura sand. The micro-CT images of the fiber reinforced cemented sand specimens were visualized in horizontal and vertical sections. Scans were obtained using a frame rate of two frames and an exposure time of 500 milliseconds. The number of images was set to optimize and typically resulted in approximately 3000 images. Then, the angles of the fibers for horizontal sections and in vertical section were calculated using the VGStudio MAX software. The number of fibers intersecting horizontal and vertical sections are counted using these images. A similar approach was used for physically cut specimens. The variation of results of fiber orientation between micro-CT scans and visual count were approximately 4-8%. The micro-CT scans were able to precisely investigate the fiber orientation distribution of fibers in these samples. The results show that 85-90% of the PVA fibers are oriented between $\pm 30^{\circ}$ of horizontal, and approximately 95% of fibers have an orientation that lies within $\pm 45^{\circ}$ of the horizontal plane. Finally, a comparison of experimental results with the generalized fiber orientation distribution function $\rho(\theta)$ is presented for isotropic and anisotropic distribution in fiber reinforced cemented Toyoura sand specimens. Experimentally, it can be seen that the average ratio of the number of fibers intersecting the finite area on a vertical plane to number of fibers intersecting the finite area on a horizontal plane (N_{tot}^{V} /N_{tot}^{H}) cut through a sample varies from 2.08 to 2.12 (an average ratio of 2.10 is obtained in this study). Based up on the analytical predictions, it can be seen that the average $\mathrm{N_{tot}^{V}}$ /$\mathrm{N_{tot}^{H}}$ ratio varies from 2.13 to 2.17 for varying n values (an average ratio of 2.15).

Keywords: fiber orientation distribution; fiber reinforced; micro-CT scans; Toyoura sand

1. Introduction

In reinforcement applications, the contribution of fibers to the strength of fiber-reinforced soils is dependent on the orientation of the fibers. Fibers mainly offer their contribution when subjected to tension and the orientation of the fibers within a specimen is therefore found to be particularly important for the strength of reinforced soils (Michalowski and Cermak 2002). Fibers are in general most influential when orientated in the same direction as the tensile strains (Diambra 2010). Fibers that contribute most to strength are those with an orientation in the direction of maximum specimen extension (Michalowski and Cermak 2002, Michalowski 1997, Michalowski 2008). The random fiber orientation has been deemed most effective as it will not create planes of weakness in the sample during shearing (Schmidt 2015, Safdar 2018, Safdar *et al.* 2020).

Fig. 1 shows the stress-strain behavior of rigid steel fiber reinforced sand under various fiber orientation conditions. It can be seen that the maximum extension occurs in the horizontal plane. Therefore, the contribution of the horizontal fibers is the largest. In a specimen with randomly distributed fibers, a portion of the fibers is compressed, and a portion is subjected to extension (of varying intensity). Consequently, the overall contribution of these fibers to strength is less than that of the horizontal fibers with the same fiber concentration. Since the domain of tensile strains varies with the loading conditions, it is impossible to universally define an optimum fiber orientation; the most desirable fiber orientation is obviously related to the particular geotechnical application and the working conditions. However, it is of particular interest to find methods for controlling or, at least, for assessing the distribution of fiber orientations induced by a certain mixing and sample formation procedures (Diambra 2010).

Gao and Zhao (2013) presented the relevance of fiber orientation distribution in practical geotechnical applications (e.g., slope stability) and stated that the reinforcing effect is strongly dependent on the relative orientation between the loading direction and the preferred fiber orientation. In addition, they suggested that special attention should be paid to optimal placement of the fibers during construction. As an example, Fig. 2 shows as a schematic of optimal fiber orientation for stabilization of an inclined slope with fibers. The preferred fiber orientation plane is assumed to be parallel to the out-of-plane direction.

The stress state for a soil element along the failure surface at various depths can then be described by the angle between the major principal stress direction (σ_1) and the

*Corresponding author, Assistant Professor
E-mail: drsafdar@uetpeshawar.edu.pk
[a]Associate Professor

ISSN: 2005-307X (Print), 2092-6219 (Online)

vertical direction (ξ). The example of a homogeneous slope with a potential slip surface shown in Fig. 2 can be taken as an illustration of the importance of the orientation of fiber and major principal stress direction on the potential failure plane in a homogeneous soil slope.

The fibers in the direction of the largest extension contribute most to the strength of the composite, whereas the fibers under compression can have an adverse effect on the composite stiffness, and do not produce an increase in the composite strength (Michalowski and Cermak 2002). Fiber orientation also affects the mechanical response due to its interaction with soil particles at micro-mechanical level. Randomly oriented fibers have been found to be effective in improving the strength of soils by friction and coiling around the soil particles. Fibers are most influential when orientated in the same direction as the tensile strains for any particular loading condition (Salah-ud-din 2012). In laboratory testing and the field/practical applications, the distribution of fibers can usually be characterized by a preferred plane of fiber orientation (Michalowski and Cermak 2002, Diambra *et al.* 2007, Shukla 2017).

Kanchi *et al.* (2014) studied the effect of anisotropic distribution of fibers on the stress-strain response of the reinforced soil and an analytical model was formulated for the fiber reinforced soil. The results showed that, as the inclination of fibers with the horizontal plane increased, the contribution of fibers in improving the strength of fiber reinforced soil decreased. The effect of fibers was found to be maximum when they were in the direction of extension, and vice versa. Li *et al.* (2016) conducted a laboratory study to investigate the effect of randomly distributed discrete fiber on the mechanical properties of microbial induced calcite precipitation (MICP) treated soil and discovered the corresponding mechanisms. The results showed that remarkable improvements in shear strength, ductility, and failure strain were achieved with fiber addition in the MICP-treated sand. Choi *et al.* (2016) presented a study on the use of polyvinyl alcohol (PVA) fibers and biocement to improve the engineering properties of Ottawa silica sand.

The testing results indicated that the use of fibers facilitated the MICP process in sand by bridging the pores in sand particles. As a result, the unconfined compressive strength and the splitting tensile strength of the biocemented, fiber reinforced sand increased by 138% and 186%, respectively; the permeability reduced by 126%, and the brittleness (expressed as the ratio between unconfined compressive strength and splitting tensile strength) was reduced by a half when compared with those of untreated sand. The splitting tensile strength and splitting secant elastic modulus increased with increasing in either calcium carbonate content or fiber ratio. The use of PVA fibers together with MICP treatment could also increase the failure strain and the post-failure splitting tensile strength (Choi *et al.* 2019). Wood *et al.* (2016) proposed a constitutive model to clarify a few aspects of the response of the fiber reinforced soils: the influence of fibers on the volumetric behaviour; the existence and nature of asymptotic states; and the stress-dilatancy relationship. Ghadr and Bahdori (2019) reported that the contribution of fibers to the strength of fiber reinforced soils is dependent

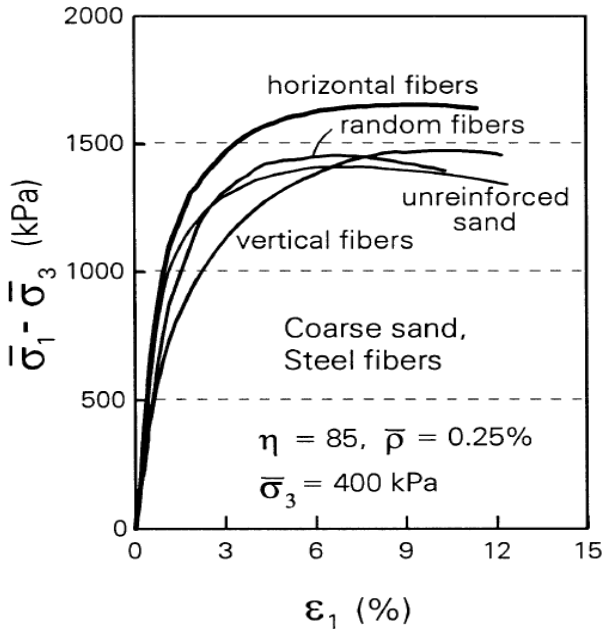

Fig. 1 Stress-strain behavior for steel fibers under various orientation conditions (Michalowski and Cermak 2002)

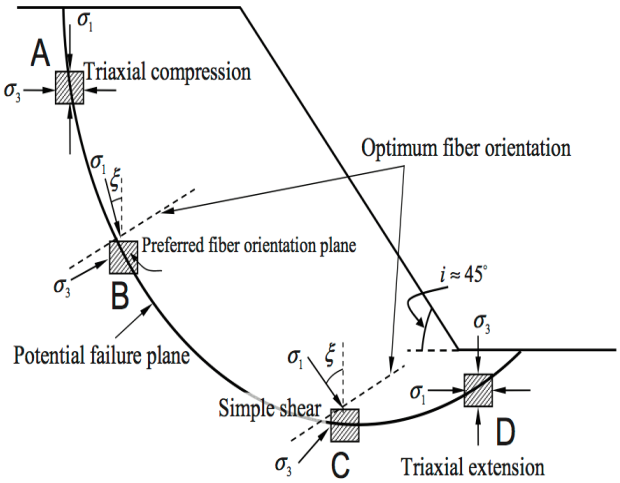

Fig. 2 Schematic of optimal fiber orientation for stabilization of a slope with fibers (Gao and Zhao 2013)

on multiaxial stress space. The study further investigated the dependency of steady states on anisotropy in unreinforced and reinforced (with 1.5% micro-synthetic fibers) well-sorted sands with different shape and size properties. Further studies on the fiber reinforced sand related to liquefaction potential (Sonmezer 2019), effect of strain level on the strength evaluation (Bahrami and Marandi 2020) and indirect measurement of shear strength parameters using laboratory tests and intelligent systems (Armaghani *et al.* 2020) are recently reported.

In laboratory, the normal procedures for sample preparation of fiber reinforced sand generally produce a distribution of fiber orientations with a preferential bedding orientation, generating strength anisotropy of the composite's response under loading. While demonstrating the potential application of X-ray tomography to the

Table 1 Testing program for studying the fiber orientation distribution (FOD)

Test No.	Test ID	Length of fibers [mm]	Diameter of fibers [mm]	Cement Content [%]	Fibers Content [%]
1	FOD-C2F0.5M0	12	0.11	2	0.5
2	FOD-C2F1M0	12	0.11	2	1
3	FOD-C2F2M0	12	0.11	2	2

analysis of fiber reinforced soils (Soriano *et al.* 2017). Therefore, it is important to investigate the orientation of fibers across single element test specimens. The following testing program was designed to investigate the fiber orientation distribution in the triaxial tests conducted in this study, to determine if there are any artefacts due to the preparation methods.

2. Testing overview

Two forms of image analysis were performed on PVA fiber reinforced cemented Toyoura sand specimens to study the fiber orientation distribution (FOD) of the fibers. Table 1 summarizes the testing program used to evaluate the FOD of the specimens. Two approaches were used for validation purposes:

1) Micro-CT technique with image analysis;
2) Image analysis of physically cut specimens with coloured fibers.

2.1 Sample preparation

Samples with of 50 mm diameter and height of 100 mm were prepared in a polyvinyl chloride (PVC) mold to a target dry density value (e.g., ρ_d = 1.489 g/cm^3) using the under-compaction moist tamping technique (Ladd 1978). Three mixtures of fiber reinforced cemented Toyoura sand samples were prepared with 10% moisture, 2% cement, and 0.5-2% (0.8-3.2% volumetric concentration) coloured fiber contents by mass and compacted in 5 layers (each 20 mm) as per the other studies in this study. Samples were then cured for 7 days to avoid any disturbance during the transportation of the samples to the testing equipment.

2.2 Micro-CT scanning

Computerized Tomography (CT) scans were performed at the Department of Sustainable Archaeology, Western University using a Nikon Metrology, Inc. micro-CT scanner with voxel resolution of approximately 50-60 μm. Fig. 3 shows the micro-CT Scanner used for the investigation of the fiber orientation distribution (FOD) and Fig. 4 shows horizontal and vertical sections of the fiber reinforced cemented Toyoura sand specimen obtained using the micro-CT scanner. Scans were obtained using a frame rate of two frames and an exposure time of 500 milliseconds. The

Fig. 3 Micro-CT scanner used for fiber orientation distribution (Located at the Department of Sustainable Archaeology, Western University) (Safdar 2018)

number of images was set to optimize and typically resulted in approximately 3000 images. Scanning time for each of the three specimens was approximately 53 minutes. The voltage was 130-140 KV and the intensity of 35-45 mico-ramps was varied in all specimens. Resolution varied from approximately 50 to 60 microns. After, scanning, the individual micro-CT radiographs were reconstructed using CT-Pro reconstruction software. Following this, the reconstructed CT Pro files were visualized using the VGStudio MAX imaging software (Klages 2013). VGStudio MAX allows the micro-CT images of fiber reinforced cemented sand specimens to be visualized in the horizontal and vertical sections. Then, the angles of the fibers for 4 horizontal sections (each 25 mm height) and in 1 vertical section (center) were calculated using the software. In addition, the number of fibers intersecting horizontal and vertical sections are also counted using the advanced CT images.

2.3 Physically cut specimens

In previous studies, the physical fiber counting procedure for each area was performed visually with the aid of digital images. Fig. 5 shows the vertical and horizontal sections of 2 specimens used for visual counting of fibers in this study (the specimen results for 2% fiber content by weight and 3.2% volumetric concentration were discarded due to the difficulty in counting fibers). This procedure is usually adopted due to the unavailability of any electronic image analysis tool which could automatically perform the counting of fibers. First, the samples are extruded from the mold and cut at 25 mm sample height using a bench-saw.

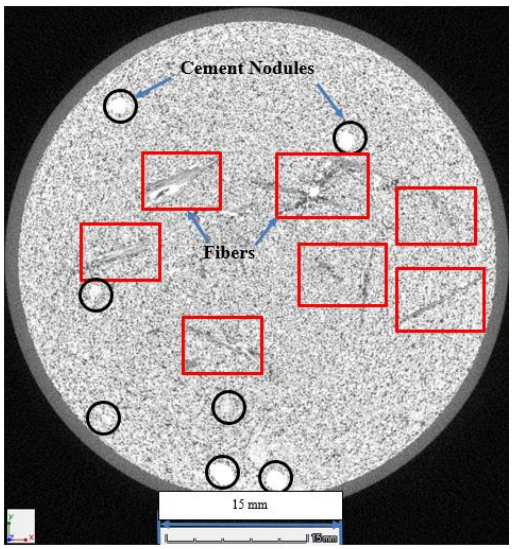

(a) Vertical section: circles show cement nodules, squares show fibres

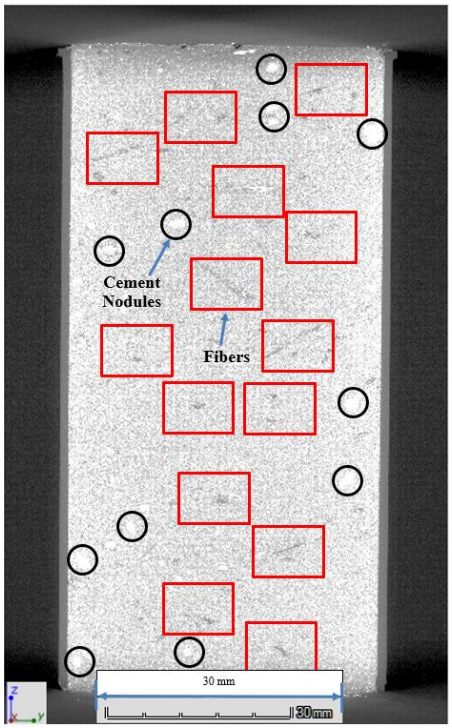

(b) Horizontal section: circles show cement nodules, squares show fibers.

Fig. 4 Micro-CT Scans (a) Vertical section (b) Horizontal section (Safdar 2018)

Fig. 5 Vertical and horizontal sections of fiber reinforced cemented Toyoura sand specimens using a thin bench-saw (Safdar 2018)

Then, images were taken using a digital camera and the counting of fibers was performed manually at each side of the section. A similar procedure was adopted in previous study (Diambra 2010).

2.4 Numerical analysis of fiber orientation

A generalized fiber orientation distribution function $\rho(\theta)$, which represents the volumetric concentration of fibers in an infinitesimal volume dV having an orientation of angle θ, was utilized for interpretation of this work. A brief description of the analytical procedure is presented below and in further detail in Diambra (2010)

$$\rho(\theta) = \overline{\rho}(A + C|\cos^n\theta|) \quad (1)$$

Where $\overline{\rho}$ is the average volumetric concentration of the fibers and is defined as the total volume of fibers (V_f) per sample volume (V)

$$\overline{\rho} = \frac{V_f}{V} \quad (2)$$

A, C and n are constants linked by the relationships

$$C = \frac{1-A}{\int_0^{\pi/2}\cos^{n+1}(\theta)d\theta} \quad (3)$$

However, there are no particular restrictions on the choice of the $\rho(\theta)$ function as long as the following Eq. (4) is fulfilled

$$\rho(\theta) = \frac{1}{V}\int \rho(\theta)dV \quad (4)$$

The fiber orientation distribution in Eq. 1 requires two of the three constants A, C and n to be specified. The procedure is simplified even further by assuming A = 0, meaning that no fibers have vertical orientation, so that only n needs to be adjusted. Table 2 presents the results for the CT scans and visual counting methods on the two samples reinforced with PVA fibers.

3. Results

The results of N_{tot}^{H} (number of fibers intersecting the finite area on a horizontal plane cut through a sample) and N_{tot}^{V} (number of fibers intersecting the finite area on a vertical plane cut through a sample) shown in Table 2 were obtained using the micro-CT scans and visual count (VC). Table 2 shows a non-uniform fiber orientation distribution along the different sections of specimens. For example, section 75 mm (a) shows a percentage variation of approximately 11% between the micro-CT scans and visual count (VC). However, it can be seen that on average 4-8% variation occurs between two samples prepared at different fiber concentration (e.g., 0.5-1%).

Table 3 shows a comparison of the results obtained from the orientation parameters (experimental investigations) and analytical predictions. Table 3 shows the non-uniform distribution of fibers along different sections of specimens between analytical predictions and using orientation parameters (experimental investigations). For example, sample C2F0.5M0 shows percent variation of

Table 2 Experimental data for studying the fiber orientation distribution (FOD)

Depth of section	**Average No. of Fibers Intersecting 50 mm ×25 mm area (CT Scan)**			**Average No. of Fibers Intersecting 50 mm ×25 mm area (Visual Count)**			**Percent Variation (%)**
	N_{tot}^{V}	N_{tot}^{H}	$\frac{N_{tot}^{V}}{N_{tot}^{H}}$	N_{tot}^{V}	N_{tot}^{H}	$\frac{N_{tot}^{V}}{N_{tot}^{H}}$	[(CT-VC/CT*100)]
FOD-C2F0.5M0							
25mm(a)	84	37	2.27	75	42	1.78	22
25mm(b)	92	49	1.88	83	45	1.84	2
50mm(a)	104	42	2.48	92	37	2.48	0
50mm(b)	121	51	2.37	98	44	2.22	6.3
75mm(a)	97	48	2.02	88	39	2.25	11
75mm(b)	117	67	1.75	105	55	1.90	8.5
100mm(a)	87	39	2.23	76	31	2.45	9.8
100mm(b)	79	35	2.26	65	27	2.40	6.2
			2.12			2.16	8.22
FOD-C2F1M0							
25mm(a)	233	92	2.53	188	81	2.32	8.3
25mm(b)	197	103	1.91	175	88	1.98	3.6
50mm(a)	169	73	2.32	157	66	2.37	2.1
50mm(b)	217	115	1.89	197	98	2.01	6.3
75mm(a)	206	87	2.37	184	77	2.38	0.4
75mm(b)	129	75	1.72	117	68	1.78	3.5
100mm(a)	147	88	1.67	132	76	1.73	3.6
100mm(b)	155	65	2.38	146	58	2.51	5.5
			2.08			2.14	4.16

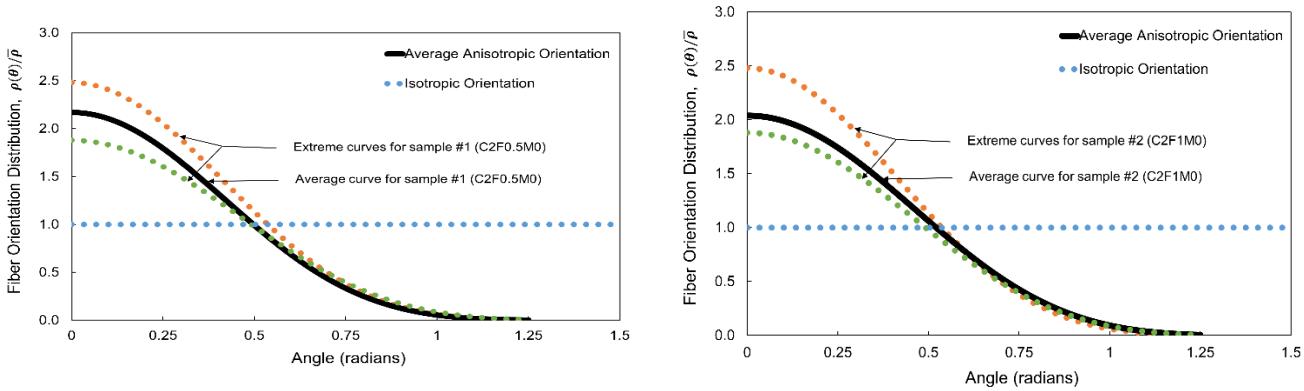

(a) 2% cement and 0.5% fiber (b) 2% cement and 1% fiber

Fig. 6 Fiber orientation distribution according to Eq. 4 for fiber reinforced cemented samples, a) C2F0.5M0 (A = 0, and n = 4), and b) C2F1M0 (A = 0, and n = 8), prepared with moist tamping technique, compared with isotropic orientation distribution (A = 1, and n = 0)

approximately 0-12% and sample C2F1M0 shows 1.3-50%. However, it can be seen that on average 5-9% variation occurs between two samples prepared at different fiber concentration (e.g., 0.5-1%).

A reasonable fit of N_{tot}^{H} and N_{tot}^{V} for the physically cut samples and analytical predictions can be seen in Table 3. The counting of fibers was performed using the VGStudio MAX software and visually for different sections of the samples is shown in Table 2. Experimentally, it can be seen that the average N_{tot}^{V} /N_{tot}^{H} ratio varies from 2.08 to 2.12 (an average ratio of 2.10 is obtained in this study). Based up on the analytical predictions, it can be seen that the average N_{tot}^{V} /N_{tot}^{H} ratio varies from 2.13 to 2.17 for varying n values (an average ratio of 2.15). Therefore, for specimen reinforced with PVA fibers (C2F0.5M0), the values of A = 0 and n = 6 (corresponding to N_{tot}^{V} /N_{tot}^{H} = 2.17) closest to the average value for moist tamped sample have been adopted due to the results obtained from

Table 3 Predicted data for studying the fiber orientation distribution (FOD)

Depth of section	Orientation Parameters using Experimental Investigations			Analytical Predictions			Percent Variation (%)
	A	n	C	N_{tot}^{V}	N_{tot}^{H}	$\frac{N_{tot}^{V}}{N_{tot}^{H}}$	[(OP-AP/OP*100)]
FOD-C2F0.5M0							
25mm(a)	0	7	2.32	81	39	2.08	10.3
25mm(b)	0	4	1.88	93	46	2.02	7.4
50mm(a)	0	8	2.46	106	43	2.46	0
50mm(b)	0	7	2.33	119	49	2.42	3.8
75mm(a)	0	5	2.04	101	46	2.19	7.4
75mm(b)	0	3	1.69	121	64	1.89	11.8
100mm(a)	0	6	2.18	91	42	2.16	0.92
100mm(b)	0	6	2.18	83	38	2.18	0
			2.13			2.17	5.2
FOD-C2F1M0							
25mm(a)	0	8	2.46	236	93	2.53	2.8
25mm(b)	0	4	1.88	201	105	1.91	1.6
50mm(a)	0	7	2.33	165	76	2.17	6.8
50mm(b)	0	4	1.88	217	112	1.93	2.6
75mm(a)	0	7	2.33	215	91	2.36	1.3
75mm(b)	0	3	1.69	137	54	2.53	49.7
100mm(a)	0	3	1.69	141	89	1.58	6.5
100mm(b)	0	7	2.33	154	67	2.29	1.7
			2.07			2.13	9.1

experimental study. For specimen reinforced with PVA fibers (C2F1M0), the values of A = 0 and n = 5 (corresponding to $N_{tot}^{V} / N_{tot}^{H} = 2.08$) closest to the average value for moist tamped sample have been adopted due to the results obtained from experimental study. It is also reported in the literature that the moist tamping technique appears to produce a $N_{tot}^{V} / N_{tot}^{H}$ ratio of about 2.11, which is independent of the average volumetric concentration of fibers for the range of fiber contents (Diambra 2010).

Fig. 6 shows the average anisotropic orientation distribution of fibers for the analyzed fiber reinforced cemented Toyoura sand specimens.

An assumed isotropic orientation distribution (A = 1) is plotted as a reference. It can be seen that 85-90% of the PVA fibers oriented between ±30° of horizontal, and approximately 95% of fibers have an orientation that lies within ±45° of the horizontal plane and only 5% of fibers lie above 45° of the horizontal plane. Similar results have also been reported in a previous study (Diambra 2010) on moist tamped fiber reinforced samples supporting the results and conclusions in this research. In addition, no layering effect was observed, and the samples were found to have a relatively uniform distribution. This might be due to scarifying the already placed layer before pouring the next one and preparing the specimens in a medium dense state. However, layering effect might occur in very loose samples.

In triaxial compression tests, a considerable increase of shear strength is contributed by the presence of fibers, while for tests conducted in extension loading conditions; the benefit of fibers is very limited. This behaviour confirms that the tamping technique in the moist condition generates preferential near-horizontal orientation of fibers, that is, the anisotropic distribution of fiber orientation (Shukla 2017).

In field applications, moist tamping sample preparation technique generally produces a soil fabric/structure that resembles that of the rolled-compacted construction fills (Diambra *et al.* 2010, Ibraim *et al.* 2012). Hence, inclusion of fibers may not result in isotropic properties of fiber reinforced soil and the use of some simplified isotropic constitutive models, may not result in accurate predictions of the benefits attributed to fibers. For cases where the predominant load is perpendicular to the preferred plane of fiber orientation, the isotropic constitutive models, in general, under-estimate the potential benefits from the fibers (Michalowski and Cermak 2002).

4. Conclusions

In this study, three micro-CT (computerized tomography) scans were performed on colored PVA fiber reinforced cemented Toyoura sand specimens to study the fiber orientation distribution (FOD) using both micro-CT technique and image analysis of physically cut specimens.

The micro-CT images of the fiber reinforced cemented sand specimens were visualized in horizontal and vertical sections. Then, the angles of the fibers for 4 horizontal

sections (each 25 mm height) and in 1 vertical section (center) were calculated using the software. The number of fibers intersecting horizontal and vertical sections are counted using these images. A similar approach was used for physically cut specimens. The variation of results of fiber orientation between micro-CT scans and visual count were approximately 4-8%. Difficulties in visual counting arose when higher fiber content (e.g., 2%) were used, as fibers tend to cluster in groups. The micro-CT scans were able to precisely investigate the fiber orientation distribution of fibers in these samples. The results show that 85-90% of the PVA fibers are oriented between $\pm 30^{\circ}$ of horizontal, and approximately 95% of fibers have an orientation that lies within $\pm 45^{\circ}$ of the horizontal plane.

Acknowledgments

The research project was financially supported by the Western Graduate Research Scholarship at the Department of Civil and Environmental Engineering, Western University, London, Ontario, Canada. The authors would also like to acknowledge the Department of Sustainable Archaeology, Western University for providing Micro-CT Scan facility.

References

Armaghani, D.J., Mirzaei, F., Toghroli, A. and Shariati A. (2020), "Indirect measure of shear strength parameters of fiber-reinforced sandy soil using laboratory tests and intelligent systems", *Geomech. Eng.*, **22**(5), 397-414. https://doi.org/10.12989/gae.2020.22.5.397

Bahrami, M. and Marandi, S.M. (2020), "Effect of strain level on strength evaluation of date palm fiber-reinforced sand", *Geomech. Eng.*, **21**(4), 327-336. https://doi.org/10.12989/gae.2020.21.4.327

Choi, S.G., Wang, K. and Chu, J. (2016), "Properties of biocemented, fiber reinforced sand", *Constr. Build. Mater.*, **120**(1), 623-629, https://doi.org/10.1016/j.conbuildmat.2016.05.124.

Choi, S.G., Hoang, T., Alleman, E.J. and Chu, J. (2019), "Splitting tensile strength of fiber-reinforced and biocemented sand", *J. Mater. Civil Eng.*, **31**(9). https://doi.org/10.1061/(ASCE)MT.1943-5533.0002841.

Diambra, A. (2010), "Fiber reinforced sands: experiments and modelling. PhD Dissertation, University of Bristol, UK.

Diambra, A., Russell A.R., Ibraim E. and Wood D.M. (2007), "Determination of fiber orientation distribution in reinforced sand", *Géotechnique*, **57**(7), 623-628. https://doi.org/10.1680/geot.2007.57.7.623.

Gao, Z. and Zhao, J. (2012), "Constitutive modeling of artificially cemented sand by considering fabric anisotropy", *Comput. Geotech.*, **41**, 57-69. https://doi.org/10.1016/j.compgeo.2011.10.007.

Ghadr, S. and Bahadori, H. (2017), "Anisotropic behavior of fiber-reinforced sands", *J. Mater. Civil Eng.*, **31**(11). https://doi.org/10.1061/(ASCE)MT.1943-5533.0002917.

Ibraim, E., Diambra, A., Russell, A.R. and Wood, D.M. (2012), "Assessment of laboratory sample preparation for fiber reinforced sands", *Geotext. Geomembranes*, **34**, 69-79. https://doi.org/10.1016/j.geotexmem.2012.03.002.

Kanchi, G.M., Neeraja, V.S. and Babu, G.L.S. (2015), "Effect of anisotropy of fibers on the stress-strain response of fiber-reinforced soil", *Int. J. Geomech.*, **15**(1). https://doi.org/10.1061/(ASCE)GM.19435622.0000392.

Klages, A.M. (2013), "A micro-CT analysis of the hominoid subnasal anatomy", Master Thesis, Western University, London, Ontario, Canada.

Ladd, R.S. (1978), "Preparing test specimens using undercompaction", *Geotech. Test. J., ASTM*, **1**(1), 16-23. https://doi.org/10.1520/GTJ10364J.

Li, M., Li, L., Ogbonnaya, U., Wen, K., Tian, A. and Amini, F. (2016), "Influence of fiber addition on mechanical properties of MICP-treated sand", *J. Mater. Civil Eng.*, **28**(4). https://doi.org/10.1061/(ASCE)MT.1943-5533.0001442.

Michalowski, R.L. (1997), "Limit stress for granular composites reinforced with continuous filaments", *J. Eng. Mech*., **123**(8), 852-859. https://doi.org/10.1061/(ASCE)07339399(1997)123:8(852).

Michalowski, R.L. (2008), "Limit analysis with anisotropic fiber-reinforecd soil", *Ge'otechnique*, 58(6), 89-501. https://doi.org/10.1680/geot.2008.58.6.489.

Michalowski, R.L. and Cermak, J. (2002), "Strength anisotropy of fiber-reinforced sand", *Comput. Geotechnics*, **29**(4) ,279-299. https://doi.org/10.1016/S0266-352X(01)00032-5.

Safdar, M. (2018), "Monotonic Stress-Strain Behaviour of Fibre Reinforced Cemented Toyoura Sand", Ph.D. Dissertation, Western University, London, Ontario, Canada. https://ir.lib.uwo.ca/etd/5622.

Safdar, M., Newson, T., Schmidt C., *et al.* (2020), "Effect of fibre and cement additives on the small-strain stiffness behaviour of Toyoura sand", *Sustainability*, 12, 10468. https://doi.org/10.3390/su122410468.

Salah-ud-din, M. (2012), "Behaviour of fiber reinforced cemented sand at high pressures", Ph.D. Dissertation, University of Nottingham, UK. http://eprints.nottingham.ac.uk/12545/1/Thesis_Salah.pdf.

Schmidt, C.J.R. (2015), "Static and Dynamic Response of Silty Toyoura Sand with PVA Fiber and Cement Additives", Master Thesis, Western University, London, Ontario, Canada.

Shukla, S.K. (2017), "Basic Description of Fiber-Reinforced Soil, In: Fundamentals of Fiber-Reinforced Soil Engineering Developments in Geotechnical Engineering", Springer, Singapore. https://doi.org/10.1007/978-981-10-3063-5_2.

Sonmezer, Y.B. (2019), "Investigation of the liquefaction potential of fiber-reinforced sand", *Geomech. Eng*., **18**(5), 503-513. https://doi.org/10.12989/gae.2019.18.5.503.

Soriano, I., Ibraim, E. and Andò, E., *et al.* (2017), "3D fibre architecture of fibre-reinforced sand", *Granular Matter*, **19**(75). https://doi.org/10.1007/s10035-017-0760-3.

Wood, D.M., Diambra, A. and Ibraim, E. (2016), "Fibres and soils: A route towards modelling of root-soil systems", *Soils Found.*, **56**(5), 765-778. https://doi.org/10.1016/j.sandf.2016.08.003.

CC